2011-03-15

Impact of a Finite-Temperature Equation of State on Neutron Stars

Christian D. Draper
Brigham Young University - Provo

Impact of a Finite-Temperature Equation of State on Neutron Stars

Christian D. Draper

A thesis submitted to the faculty of
Brigham Young University
in partial fulfillment of the requirements for the degree of

Master of Science

Dr. David Neilsen, Chair
Dr. Eric G. Hintz
Dr. J. Ward Moody

Department of Physics and Astronomy

Brigham Young University

April 2011

ABSTRACT

Impact of a Finite-Temperature Equation of State on Neutron Stars

Christian D. Draper
Department of Physics and Astronomy
Master of Science

In this research, we study how a finite-temperature nuclear equation of state suitable for astro-physical simulations impacts the oscillation modes of neutron stars. We chose the Shen equation of state (EOS) because it accurately describes both stable and unstable nuclei as well as nuclear incompressibilities [1]. I modified the existing MHD code at BYU, the HAD code, to call a look-up table for the Shen EOS for use at run time, and added a Newton-Raphson method algorithm to convert conserved variables to primitive variables. The algorithm was tested and verified by evolving a stable neutron star for several dynamical times and evolving the same star at different resolutions. The normal mode frequency of the neutron star with the Shen EOS was measured and compared to those for neutron stars with an ideal gas EOS found by Font et. al. [2]. We found that the fundamental mode of the neutron star using the Shen EOS was slightly larger than that of the ideal gas EOS. This difference is due to the Shen EOS producing stars that are stiffer, increasing the sound speed.

ACKNOWLEDGMENTS

I would like to thank all of the faculty at BYU for their guidance and assistance. In particular I would like to thank Dr. Neilsen for his patience in teaching me a difficult subject, as well Dr. Moody and Dr. Hintz for their support through the entire process.

Finally, I would like to thank Mandy for her support and pushing me to finish.

Contents

Chapter 1

Introduction

1.1   Introduction

The life of a star is determined by the battle between the crush of gravity trying to collapse the star and the force of pressure trying to explode the star. At the end of a star's life, the nuclear fuel is spent and the outward pressure from fusion drops, which leads to the core shrinking. For a star like the Sun the collapse will stop due to the quantum mechanical effects of electron pressure. This type of stellar remnant is known as a white dwarf. White dwarfs are about the size of Earth, but can contain up to one and a half times the Sun's mass. In a more massive star, the force of the electron pressure will not be enough to stop the compression of gravity. When this happens the protons and electrons are combined, creating neutrons through the process of inverse beta-decay. As this happens an object about the size of Earth is crushed to the size of a city in just a few tenths of a second. The outer layers of the star will then fall into the vacuum left by the core's sudden contraction, reaching speeds close to 75% the speed of light. When these layers strike the super dense remains of the core they are reflected back out into space, causing a supernova explosion. The remnant after this explosion is a neutron star. A neutron star is a stellar remnant that has a

mass of about two times our Sun and a radius of just 10 to 20 km.

While neutron stars have been studied for about 80 years many questions about these objects remain unanswered, such as: What is the structure of a neutron star? What is the relationship between its mass and radius? Do more exotic forms of matter appear under the incredible pressure at the center of the neutron star? What is the maximum mass of a neutron star? Many of these questions could be answered if we knew the equation of state of the neutron star. The equation of state (EOS) describes how the density, pressure and temperature of an object are related. The neutron star's structure and stiffness are a direct result of its EOS.

Although neutron stars have been observed for 50 years, these objects are too small and too distant to be resolved. Many neutron stars we have detected have been seen in the form of pulsars. Pulsars are neutron stars whose magnetic fields cause beams of radiation to flow from its magnetic poles. The rotational axis and the magnetic axis may not line up so these beams of light can sweep around, similar to the rotating lamp of a lighthouse. If the beam points toward Earth we see the light, and when it points away we don't, causing a pulsing effect. Though detections of pulsars have helped us determine an approximate radius and spin for neutron stars there are still many properties that remain a mystery.

Another visual approach to determining information about neutron stars is to look at x-ray binary systems. In these systems, a giant or supergiant star is losing mass to a compact companion, such as a neutron star or black hole. Due to the extreme acceleration of the matter as it falls onto the compact object it is superheated and begins to emit x-rays. These systems allow us to determine the masses of the compact object. Most of the neutron stars found so far have around $1.4 M_{solar}$ as has been predicted. However, the x-ray binary Vela X-1 has a neutron star with a mas of 2.27 M_{solar} [3].

One promising observational approach to learning some of the interior properties of neutron stars is to use gravitational waves. Gravitational waves are ripples in the fabric of spacetime caused

by masses moving in non-uniform ways, such as orbits of planets around a star, or asymmetric supernova explosions. One difficulty with detecting these waves is that they interact very weakly with matter. Due to the extremely small coupling between gravitational waves and matter, it is very difficult to directly detect them. Observers have indirect evidence of their existence in the PSR B1913+16 binary system, which shows a decay in orbit that matches perfectly with energy radiated by gravitational waves as predicted by general relativity [4]. In this case, as the two neutron stars orbit each other they generate gravitational radiation. This carries energy and angular momentum away from the neutron stars, causing them to slowly move closer together. These neutron stars in PSR B1913+16 are predicted to collide and merge in about 300 million years.

Gravitational waves couple weakly to matter, so intervening objects do not distort or scatter the waves and the information we receive comes pristinely from the source. Gravitational waves should allow us to constrain the nuclear EOS. The EOS determines how strongly a neutron star is bound together (which indicates when it will disrupt) , whether or not it will form an accretion disk in a merger with a compact object, and whether a merger of two neutron stars will immediately produce a black hole. If an object has a soft equation of state, it will be pulled apart some distance away from the other object, but if it is stiff it will hold together until it is much closer. When the neutron star finally disrupts, the gravitational wave signal will suddenly drop below a detectable level, which will carry information about how close its orbit was before it finally broke apart, and about how it merged with the other object.

Many exciting advancements are being made in building and improving gravitational wave detectors so that we will be able to observe gravitational waves directly. Currently, the most sensitive detector is the Laser Interferometer Gravitational-Wave Observatory, or LIGO project. LIGO hopes to have direct evidence of gravitational waves within the next couple of years. LIGO uses interferometric techniques to detect passing gravitational waves. The two LIGO facilities are located in Washington and Louisiana about 3000 km apart. Each of the facilities are set up in an L

shape with 4 kilometer arms which house a Michelson interferometer with Fabry-Perot arms. With coincident detections at both sites, the position of the source can be determined within a band in the sky. [5]

While a simple detection of gravitational waves will be important, a greater achievement will be learning how to use these signals to advance the study of physics and our understanding of the universe. The best method we have right now for detecting signals is through matched filtering, in which we create theoretical models of gravitational wave sources and extract the waveform they produce. Once the waves are detected, we will be able to compare our theoretical waves with those we actually detect to understand what is happening.

The Einstein equations that describe the geometry of space time are a set of coupled, nonlinear, partial differential equations. For astrophysical sources in strong-field gravity, there are no known analytical solutions, and the equations must be solved numerically. Thus, the calculation of theoretical waveforms requires the use of computers to model and simulate astrophysical systems.

To simulate neutron stars we need to choose an equation of state for the neutron star. A first step in modeling a neutron star is to use the ideal gas law for the EOS. Though this gives us some qualitative understanding of neutron star properties, this EOS does not adequately model nuclear matter. For more quantitative results we need to use a physical equation of state. Cold nuclear EOSs, which assume the matter is in a low energy (T=0) state, have been used in simulations to study isolated neutron stars and binary neutron stars before merger. The merger of the neutron stars, however, releases large amounts of gravitational and nuclear energy, significantly heating the material. Thus, a finite temperature EOS is required to model the binary through and after merger.

There are currently two good candidates for a finite temperature nuclear EOS that is applicable to astrophysical temperatures and pressures. First is the EOS proposed by Lattimire and Swesty. This EOS is based on the Lattimire, Lamb, Pethic, and Ravenhall compressible liquid drop model of nuclei [6]. Another good candidate is the EOS of hot dense matter suggested by Shen et. al. [1],

which is based on relativistic mean field theory [7]. Ott has used the Shen EOS to create an EOS table for a wide variety of astrophysical processes. Ott added electron pressure, and extended the table to lower densities using the Timmes EOS [8]. Ott's EOS table has been used in a few studies of neutron star and black hole mergers by Duez [9].

For my research, I modified the HAD evolution code for the full field equations in use at BYU and implemented the Shen EOS. To do this I adapted the initialization program to load values that are required for the new EOS, specifically the temperature, the electron fraction, and the density. I also adapted the evolution routine to use the new EOS by making a solver to determine new physical values at each step in the routine. Then, I produced initial data using the Shen EOS. To do this I used the LORENE code [10]. Once initial data was obtained I simulated a single neutron star, allowing it to evolve in time, to ensure that the code was working properly.

In chapter 2, I will provide the theoretical background for neutron stars including the fluid equations and the equation of state. Chapter 3 discusses the numerical techniques used at BYU to simulate neutron stars. Chapter 4 will describe the tests and results of the simulation.

1.2   Literature Review

I have discussed the importance of the EOS on the gravitational wave signature of a merging binary. Another important question is how can gravitational wave detection help us constrain the myriad proposed EOS's? Above, I mentioned the two best candidates for finite temperature EOS's for astrophysical objects; however, there are many cold, or T=0, EOS's. To date we do not have a complete model for many-bodied nuclear matter. Though we have many models, we do not have a cohesive theory that describes nuclei in atoms that can also be extended to large amounts of nuclear matter, such as neutron stars. To be able to determine the correct model we must have experimental constraints.

Shibata et. al. [11] did the first work in examining EOS effects in binary neutron star mergers in general relativity, looking at the Innermost Stable Circular Orbit. As two neutron stars orbit one another, they emit gravitational waves which carry away energy and angular momentum, causing the orbit of the neutron stars to shrink. As they spiral toward each other they will begin to orbit each other more quickly, causing the frequency of the emitted gravitational waves to increase. Once the two neutron stars are close enough they will tidally disrupt and the signal will suddenly diminish. The compactness of the neutron stars will determine at what frequency the signal will cut off. Shibata found that neutron stars that have a softer EOS, which are less compact, will disrupt at larger distances leading to higher frequencies. One interesting point is that using this technique Shibata was able to show effects from the stiffness of the core on the wave signature [12]

Though Shibata et. al.'s work examined the physical characteristics of merging binary neutron stars, they have not looked closely at ways to constrain the EOS. Read et. al. [13] has pioneered an approach which allows us to constrain the EOS from the detected gravitational wave. In this approach they compare the waveform from the inspiral of two point particles to that of extended objects, especially when they are close to the last stable orbit and the disruption. In this way they are able to constrain several parameters helping to narrow the set of possible cold EOS's. As the extended neutron stars begin to get closer their shapes elongate, changing the wave form from that of point particles. When the merger happens the disruption will also be significantly different from that of the point particles at the same orbital difference. By comparing the wave forms of many different EOSs with different characteristics to the point particle wave forms, Read has shown that it is possible to constrain the EOS and also determine the radius of the neutron star to about 1 km.

The work described above used cold nuclear EOS's. In the case of Read three different polytropes are stitched together to simulate different layers in the neutron star. A cold nuclear EOS can be written in polytropic form, but at finite temperatures different nuclear processes are available, and the EOS cannot be written in such a simple form. As mentioned previously, the two best candi-

dates for an astrophysical finite temperature EOS are the Lattimer-Swesty liquid drop model EOS and the Shen mean field model. A significant amount of work has been done modeling neutron stars and neutron star collisions in the post-Newtonian regime. In these models an approximation is made to the Einstein field equations instead of the full field equations. These approximations ignore the emission of gravitational waves and are good when the neutron stars are far apart and spacetime isn't changing dramatically. However, as the neutron stars draw near to each other, the dynamical spacetime can have significant effects on the motion of the neutron stars [14].

Recently Duez et. al. has modeled neutron star-black hole mergers using the full Einstein field equations comparing the polytropic EOS with the Shen EOS. They found that the Shen EOS caused the neutron star to fall into the black hole faster with less matter being pulled into a tidal tail and accretion disk. Though this is a start there is still much work to be done using the Shen EOS in astrophysical simulations [9].

Chapter 2

Magneto-hydrodynamic Equations

2.1   Geometry and Fluid Equations

In general relativity spacetime geometry is described by a manifold with a metric, $g_{\mu\nu}$. The Einstein equations couple the curvature of spacetime, represented here by the Einstein tensor as $\mathbf{G}$, to the mass and energy distribution of matter, represented by the stress-energy tensor, $\mathbf{T}$,

$$\mathbf{G} = 8\pi\mathbf{T}, \tag{2.1}$$

in units where $G = 1$ and $c = 1$. The Einstein tensor also satisfies the contracted Bianchi identities

$$\nabla \cdot \mathbf{G} = \mathbf{0}; \tag{2.2}$$

and the conservation of energy requires

$$\nabla \cdot \mathbf{T} = \mathbf{0}. \tag{2.3}$$

The last equation describes the equations of motion for matter, as well as the local conservation of energy and momentum.

The Einstein equations are a set of 10 coupled, second-order partial differential equations for the metric $g_{\mu\nu}$. These equations are not all independent due to the Bianchi identities which are

$$\partial_0 G^{0\nu} = -\partial_i G^{i\nu} - \Gamma^{\mu}_{\lambda\mu} G^{\lambda\nu} - \Gamma_{\lambda\mu} G^{\mu\lambda}. \tag{2.4}$$

The Einstein tensor **G** contains second order derivatives of the metric. The right hand side of the Bianchi identities therefore contain time derivatives of at most order 2. Thus, $G^{0\mu}$ can contain only time derivatives of first order. The four equations

$$G_{0\mu} = 8\pi T_{0\mu} \tag{2.5}$$

are four constraint equations, and the other 6 equations

$$G_{ij} = 8\pi T_{ij} \tag{2.6}$$

are evolution equations.

Simulations of astrophysical systems in general relativity usually require solving a Cauchy problem, where data are set for an initial time and then evolved forward in time to obtain the system's evolution. Solving a Cauchy problem requires a separation between space and time, which are linked in general relativity. Arnowitt, Deser, and Misner (ADM) created a 3+1 formulation of the Einstein equations which separates spacetime into spacelike foliations pieced together along a timelike vector. The hypersurfaces are parametrized by a global time parameter and are connected to each other by a lapse function α and a shift vector β^i. The ADM metric is

$$ds^2 = -(\alpha^2 - \beta_i \beta^i)dt^2 + 2\beta_i dt dx^i + h_{ij} dx^i dx^j, \tag{2.7}$$

where the lapse, α describes the proper time between the two hypersurfaces normal to the surface. The shift, β^i, describes how the coordinate x^i changes from hypersurface to hypersurface. The 3-metric h_{ij} is defined as the projection of the metric $g_{\mu\nu}$ onto each spacelike hypersurface. The extrinsic curvature tensor K_{ij}, describes the curvature of each individual hypersurface. In our simulations, we will not evolve the spacetime.

We model neutron stars as perfect fluids with a finite-temperature nuclear EOS. A perfect fluid is a fluid with an isotropic pressure and no viscosity or heat conduction. The stress-energy tensor for the perfect fluid is

$$T_{ab} = h_e u_a u_b + P g_{ab}. \tag{2.8}$$

In this equation u_a is the four velocity of the fluid, h_e is the enthalpy, and P is the pressure. We define the enthalpy as

$$h_e = \rho_0 + \rho_0 \varepsilon + P, \tag{2.9}$$

where ρ_0 is the rest energy density and ε is the specific internal energy.

We define the Lorentz factor, $W = -n^a u_a$, between the fluid frame and the fiducial ADM observers, and then $v^i = \frac{1}{W} h^i_j u^j$ is the fluid velocity in the frame of the ADM observers. The variables ρ_0, v^i, and P, are known as the primitive variables, to distinguish them from the conserved variables defined below.

Numerical methods for compressible fluids with shocks are based on the work of Godunov [15], using the integral conservation laws for the fluid. To write the fluid equations in conservation form, we introduce the conserved variables, D, S_i and τ which are defined as

$$D = W \rho_0, \tag{2.10}$$

$$S_i = h_e W^2 v_i, \tag{2.11}$$

$$\tau = h_e W^2 - P - D. \tag{2.12}$$

These variables correspond to baryon density, momentum and the kinetic energy in the classical limit. In general spacetimes, it is convenient to introduce the densitized variables

$$\widetilde{D} = \sqrt{h} D \tag{2.13}$$

$$\widetilde{S}_i = \sqrt{h} S_i \tag{2.14}$$

$$\widetilde{\tau} = \sqrt{h} \tau. \tag{2.15}$$

This allows us to write the fluid equations in balanced law form [16], as seen in equation 2.3 above,

$$\partial_t \widetilde{D} + \partial_t [\alpha \widetilde{D}(v^i - \frac{\beta^i}{\alpha}] = 0 \tag{2.16}$$

$$\partial_t \widetilde{S}_j + \partial_t [\alpha(S_j(v^i - \frac{\beta^i}{\alpha}) + \sqrt{h}Ph^i{}_j)] \tag{2.17}$$

$$= \alpha^3 \Gamma^i{}_{jk}(\widetilde{S}_i v^k + \sqrt{h}Ph_i{}^k) + \widetilde{S}_a \partial_j \beta^a - \partial_j \alpha(\widetilde{\tau} + \widetilde{D})$$

$$\partial \widetilde{\tau} + \partial_i [\alpha(\widetilde{S}^i - \frac{\beta^i}{\alpha}\widetilde{\tau} - v^i \widetilde{D})] = \alpha[K_{ij}\widetilde{S}^i v^j + \sqrt{h}KP - \frac{1}{\alpha}\widetilde{S}^a \partial_a \alpha] \tag{2.18}$$

where ${}^3\Gamma^i{}_{jk}$ is the Christoffel symbol associated with the 3-metric h_{ij} defined on each of the ADM hypersurfaces, and K is the trace of the extrinsic curvature, $K = K^i{}_i$. To close the system we choose an equation of state.

2.2 Equations of State

As mentioned in Chapter 1, the ideal gas law equation of state is used most often due to its simplicity. In this EOS the pressure, P, is directly proportional to the internal energy, ε,

$$P = \rho_0 \varepsilon (\Gamma - 1), \tag{2.19}$$

where Γ is the adiabatic constant and ρ_0 is the density. Under isentropic conditions this law reduces to polytropic form with κ being the dimensional constant

$$P = \kappa \rho_0{}^\Gamma. \tag{2.20}$$

The simplicity of this EOS allows the primitive variables to be determined quickly, making it computationally inexpensive to evaluate during the evolution [17]. However, this EOS naturally has limitations in modeling dense nuclear matter. Although the ideal gas EOS can give us a qualitative picture of the neutron star dynamics, it will not give us a detailed picture of the neutron stars' structure or include effects of nuclear interactions during the merger.

The next step to more realistically model nuclear matter is to use a hybrid EOS. In a hybrid EOS we start with a cold nuclear EOS in polytropic form and add an ideal gas component to account for shock heating. The pressure in the hybrid model is split into two pieces, the cold and the thermal pressures

$$P = P_{cold} + P_{th} \tag{2.21}$$

with the cold part being piecewise polytropic. The cold EOS can be split into many different pieces. As an example the EOS can be divided between $\rho_0 < \rho_{nuclear}$ with the adiabatic exponent Γ_1 and $\rho_0 > \rho_{nuclear}$ with adiabatic exponent Γ_2. The two pieces are made smooth at the boundary causing the dimensional constant κ_2 to be a function of $\Gamma_1, \Gamma_2, \kappa_1$ and $\rho_{nuclear}$ [18]. Though this EOS mimics shock heating it does not take into account the different nuclear processes. To take this into account we use a finite temperature nuclear EOS appropriate for astrophysical objects.

The two leading candidates for a finite temperature nuclear EOS for astrophysics are the Lattimer-Swesty EOS and the Shen EOS. Both of these take into account the formation and change of atomic nuclei depending on the pressure, temperature, and other physical quantities, though they are based on different models.

The Lattimer Swesty model is based on the compressible liquid drop model. In this model, the phase of matter is determined by treating nuclei as a compressible liquid drop and then minimizing the Helmholtz free energy associated with each drop and a free nucleon gas around it. This approach has given some interesting results of different phases of nuclei as we transition from individual nuclei to a bulk mass near nuclear densities. Many studies have been done using this EOS with success [6].

I chose to use the Shen EOS [1] because it has been successful at describing many properties of nuclei. This EOS is based on the relativistic mean field theory. The relativistic mean field theory agrees with both stable and unstable nuclei of all sizes, as well as agreeing with spin properties and incompressiblities. The Shen EOS extends these ideas to uniform matter, with no heavy nu-

clei, and nonuniform matter, with heavy nuclei, under a wide range of temperatures (T), densities (ρ_0) and electron fractions (Y_e). The EOS is extended to lower densities using the Thomas-Fermi approximation. One of the interesting findings from the Shen EOS is the formation of heavy nuclei under certain conditions. At low densities the protons and neutrons form a homogeneous gas. As the density increases, heavy nuclei begin to form to minimize the free energy. As the density continues to climb, we again reach a point of uniform matter [7].

The Shen EOS is too complicated to be calculated during run time so it must be put into a table, and the software uses the table to calculate a given state using interpolation. The Shen et. al. table is too coarse to be used in on the fly interpolation for precise analysis. We have chosen to use the table refined and extended by Ott et. al. [18] To refine the table Ott used the cubic Hermite interpolation function provided by Timmes and Swesty [8] and modified to have monotonic interpolation behavior as suggested by Steffen [19]. This refines the table giving 18 points per decade in ρ, 41 points per decade in T and 50 points in Y_e. The values below T = 0.1 MeV and above T = 100 MeV were extrapolated linearly keeping the composition constant. At densities below $10^7 g/cm^3$ the Timmes EOS is used with the assumption of an ideal gas [18].

Chapter 3

Numerical Implementation

Many differential equations that arise in astrophysical systems are difficult to solve analytically, and this has spurred the need to find approximate solutions. In finite difference methods differential operators are replaced with algebraic operators, reducing differential equations to algebraic equations. This section discusses numerical techniques used to evolve the perfect fluid equations.

3.1   Evolution Code

The HAD code that evolves the perfect fluid equations is a high resolution shock capturing scheme based on the PPM reconstructions and HLLE numerical flux. The fluid equations are written in balance law form with $\mathbf{u}$ as a state vector, $\mathbf{f^k}$ as flux functions and $\mathbf{s}$ as source terms we have

$$\partial_t \mathbf{u} + \partial_k \mathbf{f^k}(\mathbf{u}) = \mathbf{s}(\mathbf{u}) \tag{3.1}$$

The fluid equations are discretized using finite differences as required. I have shown in chapter 2 that the densitized conserved variables have been placed in this form.

To discretize the balance law equations we use the method of lines, discretizing space and time

separately. The one dimensional discretized form is

$$\frac{d\mathbf{u_t}}{dt} = -\frac{\hat{f}_{t+\frac{1}{2}} - \hat{f}_{t-\frac{1}{2}}}{\Delta x} + \mathbf{s}(\mathbf{u_t}) \tag{3.2}$$

where $\hat{f}$ is the consistent numerical flux. The HAD code uses the HLLE flux.

$$\mathbf{f}^{HLLE} = \frac{\lambda_r^+ \mathbf{f}(\mathbf{u}^l) - \lambda_l^- \mathbf{f}(\mathbf{u}^r) + \lambda_r^+ \lambda_l^- (\mathbf{u}^r - \mathbf{u}^l)}{\lambda_r^+ - \lambda_l^-}, \tag{3.3}$$

where

$$\lambda_l^- = min(0, \lambda_l) \tag{3.4}$$

$$\lambda_r^+ = max(0, \lambda_r). \tag{3.5}$$

The HLLE flux [20] is a central-upwind flux using the maximum characteristic velocities for both left- and right-moving waves. The characteristic velocities for the relativistic perfect fluid in the x-direction are [17]

$$\lambda_0 = \alpha v^x - \beta^x \tag{3.6}$$

$$\lambda_\pm = \frac{\alpha}{1 - v^2 c_s^2} \Big\{ v_x(1 - c_s^2) \pm \tag{3.7}$$

$$c_s \sqrt{(1 - v^2)[h^{xx}(1 - v^2 c_s^2) - v^x v^x (1 - c_s^2)]} \Big\} - \beta^x$$

Both λ's are functions of the sound speed, c_s, which must be taken from the EOS. In our case it is supplied by the EOS table, though we need to convert to relativistic speed of sound. To do this we divide c_s from the table by $h\rho_0$ the relativistic enthalpy. The point valued fluxes are then converted into numerical fluxes. The PPM is used to calculate the numerical fluxes and has been found to be less dissipative than the CENO scheme, and seems to give superior reconstruction of the stellar interior.

3.2   Conserved to Primitive Reconstruction

Using the method of lines we are able to evolve the conserved variables from initial data at time t to the advanced time $t + \Delta t$. However, we are then left to calculate the primitive variables at the advanced time. While the conserved variables are simple algebraic functions of the primitive variables, the inverse transformation is transcendental, and we must employ an iterative root finding technique. We chose to use the Newton-Raphson method to iterate an equation for the pressure which works for EOS's of the type $P = P(\rho_0, \varepsilon, Y_e)$ [21]. This is the form of the table of the Shen EOS provided by Ott.

We use the Newton-Raphson method to find a solution to the transcendental equation,

$$f = \bar{P} - P(\bar{\rho}_0, \bar{\varepsilon}, Y_e). \tag{3.8}$$

by varying a guess for the pressure, $\bar{P}$. The initial guess for the Newton-Raphson solver is the pressure from the previous time step. Using the guess for $\bar{P}$, we calculate

$$\bar{W} = \frac{\tau + \bar{P} + D}{\sqrt{(\tau + \bar{P} + D)^2 - S^2}}, \tag{3.9}$$

where $S^2 = S^i S_i$. We then calculate Y_e, ρ_0 and ε as

$$Y_e = (DY_e)/D, \tag{3.10}$$

$$\bar{\rho}_0 = \frac{D}{\tau + \bar{P} + D} \sqrt{(\tau + \bar{P} + D)^2 - S^2}, \tag{3.11}$$

$$\bar{\varepsilon} = D^{-1}(\sqrt{(\tau + \bar{P} + D)^2 - S^2} - \bar{P}\bar{W} - D). \tag{3.12}$$

The barred variables are all based on the guess for the pressure, $\bar{P}$.

The Newton-Raphson solver requires the derivative of f with respect to $\bar{P}$ which is given by

$$f' = 1 - \left.\frac{\partial P}{\partial \rho_0}\right|_\varepsilon \frac{\partial \rho_0}{\partial \bar{P}} - \left.\frac{\partial P}{\partial \varepsilon}\right|_{\rho 0} \frac{\partial \varepsilon}{\partial \bar{P}}. \tag{3.13}$$

In this equation, the terms $\left.\frac{\partial P}{\partial \rho_0}\right|_{\varepsilon}$ and $\left.\frac{\partial P}{\partial \varepsilon}\right|_{\rho 0}$ must be supplied by the EOS, and

$$\frac{\partial \rho_0}{\partial \bar{P}} = \frac{DS^2}{\sqrt{(\tau + \bar{P} + D)^2 - S^2}(\tau + \bar{P} + D)^2} \tag{3.14}$$

$$\frac{\partial \varepsilon}{\partial \bar{P}} = \frac{\bar{P}S^2}{\rho((\tau + \bar{P} + D)^2 - S^2)(\tau + \bar{P} + D)}. \tag{3.15}$$

If the determined P is not within tolerance then it is set as the guess for the next iteration of the solver. When the root has been found within tolerance the solver stops and returns values for P, ρ_0 and ε. Once a value of P has been determined the other primitive variables may also be determined

$$\rho_0 = \frac{W}{D} \tag{3.16}$$

$$v_i = \frac{S_i}{h_e W^2} \tag{3.17}$$

where h_e is given by equation 2.8 [21].

3.3 Physical Constraints

A physical solution for the primitive variables must satisfy certain constraints, namely $\rho_0 > 0$, $P > 0$ and $v^2 < 1$. Unfortunately, numerical error in the evolution algorithm can sometimes result in states at the advanced time that are unphysical. These unphysical states often cause the primitive variable solver described above to fail. To help alleviate these problems, we apply a floor to the conservative variables D and τ such that $D > \delta$ and $\tau > \delta$, for a vacuum level δ. The value of δ is typically 10^{-8} for the variables done here, and it is chosen to be small enough that its value does not affect the evolution.

After P has been determined through the Newton-Raphson routine, we check for physicality be testing if $P > 0$ and $W \geq 1$. If either of these checks fail, we flag the point and determine a physical solution by interpolation from points around it. As long as there are few errors, the code will be able to continue. If too many points fail, there may be no physical solution so the simulation terminates.

Chapter 4

Tests and Data

This section describes the initial tests of the MHD code using the Shen EOS. These tests involved evolutions of neutron stars on a fixed background geometry. Fixing the geometry is also known as the Cowling approximation.

4.1   Tests

The neutron star initial data was generated using the Nrotstar package in LORENE, a C++ library used for solving initial value problems in numerical relativity. The equation of state information is put into a table of values in number density, $\rho_0(1 + \varepsilon/c^2$ (the total density), and pressure [10]. To generate this table, we fixed the temperature of the neutron star to be $T = 1.16x10^9K$ and set the electron fraction to be $Y_e = 0.1$. We then extracted a line of data (fixed in T and Y_e) from the Shen table. The neutron star we simulated had a target mass of 1.4 M_{solar}, an enthalpy of 0.84 m^2/s^2 and no rotation. The neutron star solution from LORENE had a baryonic mass of 1.377 M_{solar} a radius of 12.245 km, a compactness of $m/r = 0.11$, and no rotation.

After producing neutron star initial data, we began tests to ensure the robustness, accuracy, and convergence of the new primitive solver for the Shen EOS. To test the robustness of the solver,

we first lowered the temperature in a small region at the center of the neutron star to the vacuum levels. This method checked the effects of abrupt density changes as well as the ability of the new routines to handle shocks and speeds approaching the speed of light. As expected, the fluid flow at the middle of the neutron star reached speeds close to the speed of light. The solver could determine physical solutions during the entire simulation, which confirms that the code is able to handle shocks and other abrupt phenomena.

To test the accuracy of the code, we evolved a single neutron star for many dynamical times to ensure that the neutron star was stable and that the average density did not increase or decrease in time. A dynamical time is the time it takes for information at the surface of the neutron star to reach the center of the neutron star and back, and can be measured from the oscillations of the density at the center of the neutron star. The evolution progressed to 9500 time steps or 3.657 ms. The simulation used 100 points across the neutron star. The average computational time for one time steps was 4.5 min. We ran the simulation on 64 processors at the Fulton Supercomputing Lab at BYU. The neutron star showed regular pulsations without significantly increasing or decreasing its average maximum density. We note that these data were treated inconsistently, as discussed below.

The final test examined the convergence at different resolutions (see fig. 4.1). In addition to the neutron star with 100 points across the neutron star mentioned above, we evolved a second neutron star with 200 points. This evolution was evolved for 2600 steps on 96 processors. The central density of the neutron star is also plotted in fig. 4.1. As seen in the figure there was a large change in density of the fine-grid neutron star. This was unexpected, as the density variations on a finer resolution should be smaller than on a coarse resolution. As we looked into this, we found that there is a problem in the code in converting units from the LORENE initial data to the geometric units used in HAD. In particular the unit transformation from LORENE units to HAD's geometric units was not consistent with the transformation from geometric units to cgs
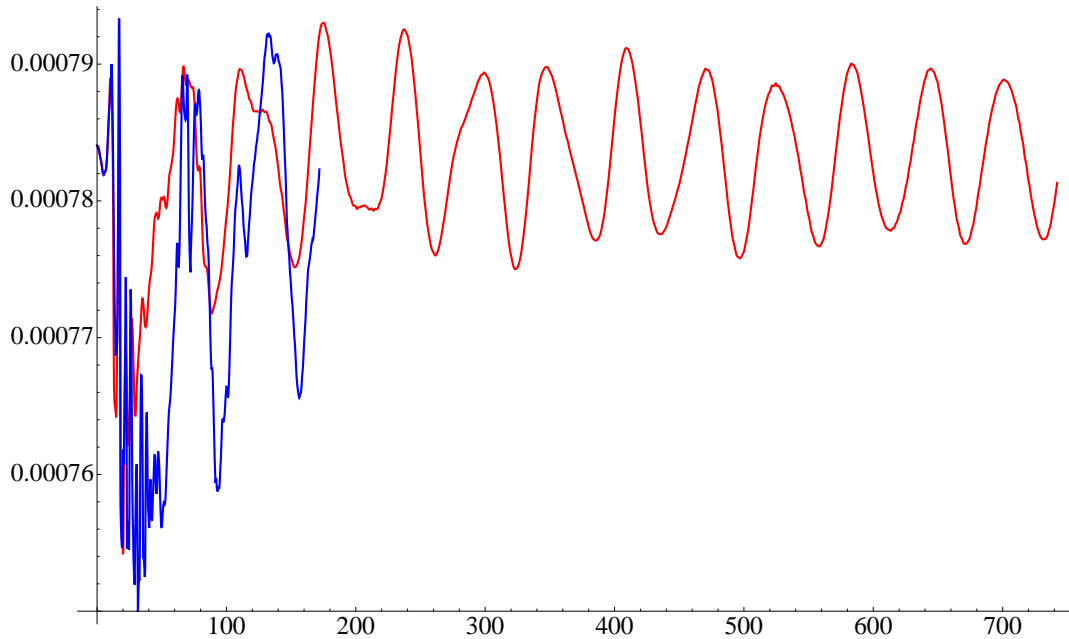
Figure 4.1 The fluctuations of the central density of two neutron star simulations. The red line is for a neutron star on a coarse grid with 100 points across the neutron star. Blue is for the finer resolution with 200 points across the neutron star. The axes are time, t, in and density, ρ_0. We see a lot of noise at the start of the simulation. This is due to a unit conversion problem that we found in the code that causes significant perturbations of the neutron stars. After about 2 ms the red signal stabilizes. The blue curve appears to be converging toward the solution found in the red, but has not had enough time to do so.

units used in the evolution code. It appears that large changes in density of the simulated neutron star occur as the neutron star transitions from the equilibrium state described by the initial data to an equilibrium that agrees with the units as they appear in HAD. After about 2 ms the code has found a new equilibrium and continues to evolve as it should. The fine grid neutron star simulation lasted for only 1 ms and so did not reach the new equilibrium. However, it appears that the large jumps in the density were becoming less and likely would have led to a new stable solution which converged with the coarse grid neutron star. In any case, these evolutions are not of equilibrium neutron stars but neutron stars with significant perturbations. This explains the apparent lack of convergence shown in figure 4.1.

4.2   Data

We were interested in how the central density of the neutron star changed over time. As mentioned above, initially there was a fair amount of noise, as the neutron star transitioned to an equilibrium position due to the unit conversion problem. This problem with units exited radial pulsations in the neutron star, related to the radial modes. If the pulsations are driven only be truncation error, then they should diminish with increasing resolution, which shows that the amplitude of these oscillations carry no physical information. However, the frequencies of the modes excited by these perturbations are a physical property of neutron stars, which can then be compared to different models. Using Fourier analysis we were able to determine the modes of the oscillations (see fig. 4.2). We found that the simulated neutron star has a fundamental frequency of 3.4 kHz, the first harmonic of 6.0 kHz, and the second harmonic of about 9.7 kHz. Given the short evolution time, the higher frequencies have large uncertainties.

Font et. al. used the ideal gas EOS with a polytropic index $n = 1$ with $\Gamma = 2$, in the Cowling approximation. This led to a neutron star with a compactness of $m/r = 0.15$ [2]. The radial modes from Font, 2.7 kHz, 4.5 kHz, and 6.3 kHz (see table 4.1) are slightly lower than those found using the Shen EOS. The Shen EOS produces neutron stars that are stiffer, with our neutron star having a compactness of $m/r = 0.11$. This leads to a neutron star that is bound together more strongly, increasing the speed of sound in the neutron star, leading to higher frequencies.
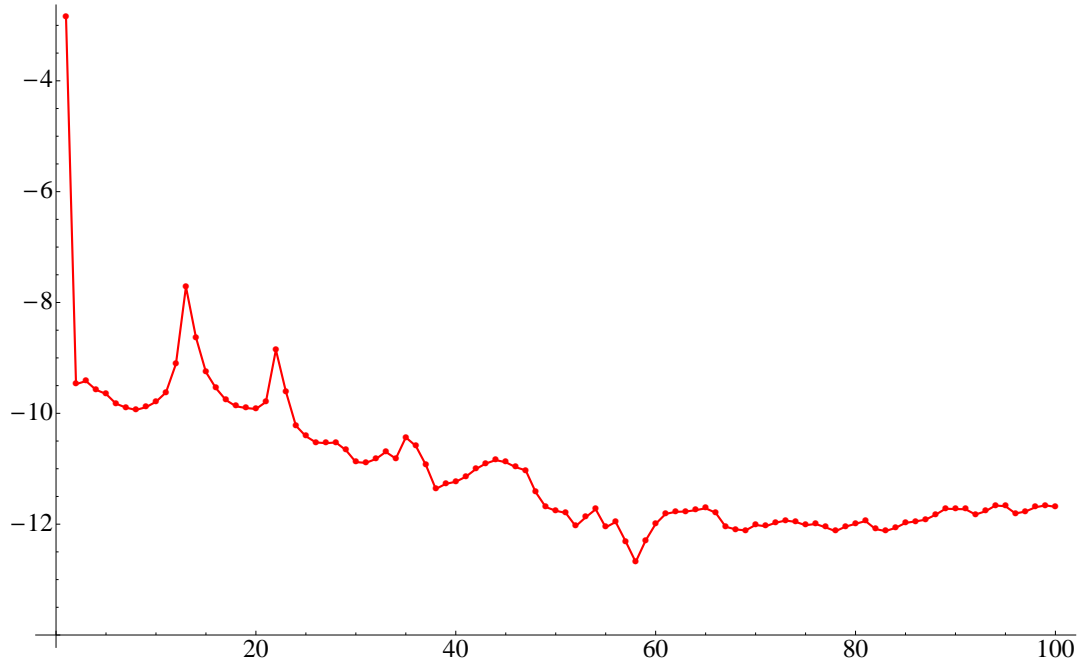
Figure 4.2 The power spectrum of the density oscillations of the coarser of the two neutron star simulations. We see peaks corresponding to oscillation frequencies at 3.4 kHz, 6.0 kHz, and 9.7 kHz. Given the limited data the uncertainty in the higher modes is large.

	Font	Shen
Mode	(kHz)	(kHz)
F	2.7	3.4
H1	4.5	6.0
H2	6.3	9.7

Table 4.1 Comparison of the frequencies of radial pulsations of two simulated neutron stars on a fixed spactime. One using the polytropic EOS with polytropic index $\Gamma = 2$ taken from [2], the other from our simulations using then Shen EOS. We show the fundamental, F, and the first and second harmonic, H1 and H2 respectively.

Chapter 5

Conclusion

I have implemented the Shen EOS into the HAD code at BYU. I wrote a conserved variable to primitive variable solver which uses the Newton-Raphson method to solve the transcendental equations. I also modified the program to do a table look-up for the Shen EOS since it is too complicated to be determined at run time.

After implementing the new routines we tested the program for robustness, accuracy, and convergence. During the test for convergence we determined that the unit conversion between the initial data, the HAD code, and the EOS table was inconsistent. This inconsistency was small, and was not noticed in the initial simulations. While this error was found after the runs for this thesis were completed, it demonstrates the importance of convergence testing to find subtle errors many different errors in the code.

From the simulations we produced, we find that the Shen EOS produces stiff neutron stars with a compactness of $m/r = 0.11$. We calculated the frequencies of radial oscillations of the neutron star by taking the Fourier transform of the central density as a function of time. The frequencies of the modes of a neutron star with the Shen EOS are slightly higher than those of a star with the ideal gas EOS. This was expected as the Shen EOS star is stiffer than neutron stars produced using the ideal gas EOS.

After correcting the unit conversion for the initial data, we can then begin looking at mergers of two neutron stars using the Shen EOS, to see how these mergers differ from those of neutron stars with other EOSs. We will also simulate neutron star-black hole mergers to see if there is a difference in the formation of an accretion disk around the black hole after the merger. We will also extract the gravitational wave signature to see how the cut-off frequency changes due to the change in the EOS.

Bibliography

[1] H. Shen, H. Toki, K. Oyamatsu, and K. Sumiyoshi, "Relativistic Equation of State of Nuclear Matter for Supernova and Neutron Star," Nucl. Phys. **A637,** 435–450 (1998).

[2] J. A. Font *et al.*, "Three-dimensional general relativistic hydrodynamics. II: Long-term dynamics of single relativistic stars," Phys. Rev. **D65,** 084024 (2002).

[3] H. Quaintrell *et al.*, "The mass of the neutron star in Vela X-1 and tidally induced non-radial oscillations in GP Vel," Astron. Astrophys. **401,** 313–324 (2003).

[4] J. M. Weisberg and J. H. Taylor, "Relativistic Binary Pulsar B1913+16: Thirty Years of Observations and Analysis," ASP Conf. Ser. **328,** 25 (2005).

[5] CalTech and MIT, "Laser Interferometer Gravitational Wave Observatory," http://www.ligo.caltech.edu/ (Accessed April 15, 2010).

[6] J. M. Lattimer and F. D. Swesty, "A Generalized Equation of State for Hot, Dense Matter," Nucl. Phys. **A535,** 331 (1991).

[7] H. Shen, H. Toki, K. Oyamatsu, and K. Sumiyoshi, "Relativistic equation of state of nuclear matter for supernova explosion," Prog. Theor. Phys. **100,** 1013–1031 (1998).

[8] F. X. Timmes and D. Arnett, "The Accuracy, Consistency, and Speed of Five Equations of State for Stellar Hydrodynamics," ApJS **125,** 277 (1999).

[9] M. D. Duez, F. Foucart, L. E. Kidder, C. D. Ott, and S. A. Teukolsky, "Equation of state effects in black hole-neutron star mergers," Class. Quant. Grav. **27,** 114106 (2010).

[10] P. O. at LUTH laboratory, "LORENE," http://www.lorene.obspm.fr/ (Accessed August 15, 2007).

[11] M. Shibata and J. A. Font, "Robustness of a high-resolution central scheme for hydrodynamic simulations in full general relativity," Phys. Rev. **D72,** 047501 (2005).

[12] K. Kyutoku, M. Shibata, and K. Taniguchi, "Gravitational waves from nonspinning black hole-neutron star binaries: dependence on equations of state," Phys. Rev. **D82,** 044049 (2010).

[13] J. S. Read *et al.*, "Measuring the neutron star equation of state with gravitational wave observations," Phys. Rev. **D79,** 124033 (2009).

[14] R. Oechslin and H. T. Janka, "Gravitational waves from relativistic neutron star mergers with nonzero-temperature equations of state," Phys. Rev. Lett. **99,** 121102 (2007).

[15] S. K. Godunov, Mat. Sb. **47,** 271 (1959).

[16] M. Anderson *et al.*, "Simulating binary neutron stars: dynamics and gravitational waves," Phys. Rev. **D77,** 024006 (2008).

[17] D. Neilsen, E. W. Hirschmann, and R. S. Millward, "Relativistic MHD and black hole excision: Formulation and initial tests," Class. Quant. Grav. **23,** S505 (2006).

[18] E. O'Connor and C. D. Ott, "A New Open-Source Code for Spherically-Symmetric Stellar Collapse to Neutron Stars and Black Holes," Class. Quant. Grav. **27,** 114103 (2010).

[19] M. Steffen, "A Simple Method for Monotonic Interpolation in One Dimension," Astron. Astrophys. **239,** 443 (1990).

[20] A. Harten and B. van Leer, "On Upstream Differencing and Godunov-type Schemes for Hyperbolic Conservation Laws," SLAM Rev. **25,** 35 (1983).

[21] C. Ott, "Stellar Iron Core Collapse in 3+1 General Relativity and The Gravitational Wave Signature of Core-Collapse Supernovae," Ph.D. thesis (University of Potsdam, Potsdam, Germany, 2007).